Computational investigation of intrinsic localization in crystalline Si

N. K. Voulgarakis, G. Hadjisavvas, P. C. Kelires, and G. P. Tsironis
Department of Physics, University of Crete and Foundation for Research and Technology-Hellas (FORTH), P.O. Box 2208, 71003 Heraklion, Crete, Greece

(Received 23 December 2003; published 23 March 2004)

We investigate numerically existence and dynamical properties of intrinsic localization in crystalline silicon through the use of interatomic Tersoff force fields. We find a band of intrinsic localized modes (discrete breathers) each with lifetime of at least 60 ps in the spectral region 548–578 cm^{-1}, located just above the zone end phonon frequency calculated at 536 cm^{-1}. The localized modes extend to more than second neighbors and involve pair central-atom compressions in the range from 6.1% to 8.6% of the covalent bond length per atom. Finite temperature simulations show that they remain robust to room temperatures or higher with a typical lifetime equal to 6 ps.

DOI: 10.1103/PhysRevB.69.113201 PACS number(s): 63.20.Ry, 05.45.−a, 63.20.Pw

In 1988 Sievers and Takeno[1] suggested that nonlinearity of interatomic forces in crystals can lead to vibrational energy localization in the form of intrinsic localized modes (ILM's) or discrete breathers (DB's) generated in the absence of any type of disorder. Subsequent theoretical analysis of this fruitful concept addressed a variety of issues[2] and in particular focused on DB rigorous existence,[3] mobility,[4] thermodynamic properties,[5] and classical and quantum[6] model systems. On the practical, experimental side, DB's have been unequivocally generated in man-made systems of micron scale such as Josephson junctions[7,8] as well as MEMS (Ref. 9) while presently only quasi-one-dimensional crystalline PtCl seems to present a clear candidate for presence of DB's on a microscopic scale.[10] From the purely computational stand point only few attempts were made so far aiming at the numerical investigation of intrinsic localization in real systems through *ab initio* or alternative numerical methods.[11–13] In the present study we perform a computationally intensive analysis that details the onset of intrinsic localization in one of the most technologically important materials, viz., in crystalline silicon, and analyze some of its properties.

Crystalline carbon, silicon, and germanium have four valence electrons and form diamond structures where each atom has four neighbors. In crystalline silicon, in particular, the nearest-neighbor distance is 2.35 Å with ground-state (cohesive) energy per atom equal to -4.63 eV while its vibrational spectrum has an upper limit band at ≈ 536 cm^{-1}. A large number of bulk, surface, as well as nanocrystalline properties can be analyzed computationally through the use of semiempirical interatomic potentials with adjustable parameters fitted from the experiment. In the present numerical study we used almost exclusively pseudopotentials of Tersoff type[14] that follow modified Morse laws while incorporation of environmental effects on bonding gives them implicit many-body character that is important in the study of several group-IV element properties.[15] Our basic aim is on one hand to investigate nonlinear localization in bulk materials, while on the other to probe at the same time the regime of validity of empirical pseudopotentials away from the usual purely linear regime. Since empirical pseudopotentials are many times used from a linear regime to melting, it is important to study in a controlled fashion their features in the vast intermediate nonlinear regime. In our computations we used a cell consisting of 216 atoms. Initially, we calculated the density of states of the linearized vibrational spectrum of Si and confirmed known results mentioned above and place the zone end boundary approximately at $\omega_\pi = 536$ cm^{-1}; possible stable ILM's can have frequencies larger than ω_π provided effective interaction hardening takes place in a range of large displacement from the equilibrium positions.

In the search for intrinsic localization properties in materials it is important to be able to construct a precise initial state that forms a breather state. We will be using a truncated Fourier domain method that has been tested and seen to work well in three-dimensional model systems.[16] Since we are seeking space localized but time periodic lattice solutions, we consider for a d-dimensional system of atoms the Fourier expansion of the atomic positions $\mathbf{R}_i$ and forces $\mathbf{F}_i$ acting on the ith atom of mass m_i in multiples of the breather frequency ω_b; we thus obtain Newton's law in the frequency domain, viz., $-m_i n^2 \omega_b^2 \tilde{\mathbf{R}}_{i,n} = \tilde{\mathbf{F}}_{i,n}$, where tilde denotes the transformed quantities and the index n labels Fourier modes. The breather construction algorithm solves iteratively this equation by assuming an initial DB frequency $\omega_b^{(0)}$ outside the phonon band as well as an initial, localized set of eigenvectors $\mathbf{R}_i^{(0)}$; these two enable the first force evaluation while through it the first mode eigenvector follows. Subsequent use of the latter corrects the frequency, obtaining thus $\omega_b^{(1)}$. Repetition of this procedure results after k iterations to

$$\tilde{\mathbf{R}}_{i,n}^{(k)} = -\frac{\tilde{\mathbf{F}}_{i,n}^{(k)}}{m_i n^2 (\omega_b^{(k-1)})^2},$$

for the first n_{max} Fourier modes except the zeroth one, while the constant zeroth mode follows from the equation $\tilde{\mathbf{F}}_{i,0}^{(k)}\{\tilde{\mathbf{R}}_{i,0}^{(k)}\} = 0$. The iterative procedure ends when there is convergence for specific values of ω_b of the breather eigenvectors $\tilde{\mathbf{R}}_{i,n}$.

Using this method we can construct three-dimensional silicon ILM's such as the one depicted in Fig. 1(a). We note

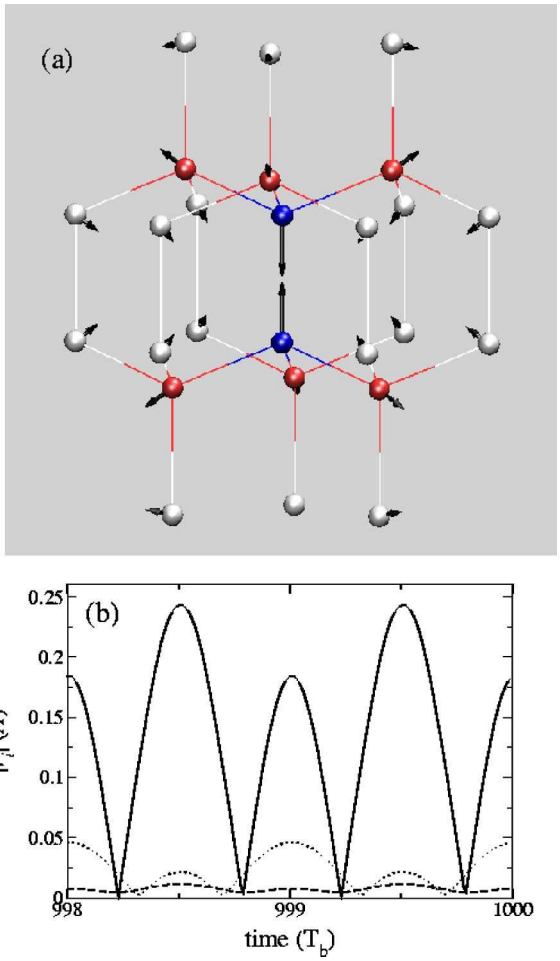

FIG. 1. (a) Numerically accurate discrete breather generation in silicon modeled by Tersoff potentials. The breather frequency is $\omega_b = 578$ cm^{-1} while vectors (magnified for visualization purposes) denote atomic displacements from equilibrium; only first (gray, red on line) and second (white) neighbors to the central (black, blue on line) two breather atoms are included. The distortion of the two central breather atoms is $a = 0.18$ Å. (b) Time evolution of the silicon breather state after 998 breather periods. We plot the absolute value of the displacements from equilibrium along the direction of motion of each atom. We note the coordinated oscillation of central (solid), first (dotted), and second (dashed) neighbor atoms.

that there are two central atoms where most ILM energy is concentrated, while each of these atoms is surrounded by three first neighboring ones oscillating in phase with their opposite to them central atom. At larger yet distances from the two central breather sites there is a layer of second neighboring silicon atoms that have smaller, yet discernible motions with the same breather frequency. We note that motion practically ceases beyond this layer of second neighbors. We thus have the typical configuration of a discrete breather thereby having a collection of atoms oscillating with the same period while the amplitude of the oscillation drops exponentially as we move away from the central oscillating sites. Using the state shown in Fig. 1(a) as initial state we performed long-time evolution of the lattice dynamics and confirmed that this localized coherent oscillating state survives to the end of the simulation, i.e., has a lifetime of at least 60 ps, or it lasts more that 10^3 DB oscillation periods at zero temperature [Fig. 1(b)].

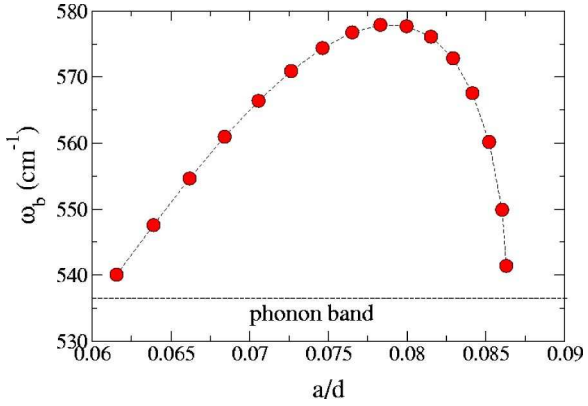

FIG. 2. (a) Breather frequency as a function of distortion of the central atoms ($d = 2.35$ Å). Dashed line corresponds to the upper limit of phonon band.

For a more systematic study of the DB properties in silicon we applied the previous approach for various breather periods; the results are shown in Fig. 2 where breather frequency is plotted as a function of the amplitude of the central atom. We observe a number of remarkable features; first we note that there is a very small zone starting at the top of the phonon band to the lowest possible breather frequency located at $\omega_{b,min} = 540$ cm^{-1} where no breathers are constructed. The lack of breathers in this small zone could be attributed to the true three-dimensional nature of the structure;[17] we also note that we find that true breather modes in the small-frequency and small-amplitude side of the breather band have weaker stability compared to the rest. In what regards the specific breather frequency-amplitude relation we observe an initial increase in DB frequency as the amplitude increases indicating an initial hardening of bonds while upon reaching a maximum in the frequency $\omega_{b,max}$ the frequency decreases with the amplitude. The presence of this second branch in the ''breather dispersion relation'' indicates the expected softening of the bonds in the breather neighborhood at even larger amplitudes.

The dynamical reasons for this distinct behavior of the intrinsically localized silicon modes arise from the potential energy of the mode central atoms as well as the specifics of the eigenvectors of each atom constituting the ILM. Indeed the nature of the pseudopotentials used in conjunction with the specific diamond structure of the silicon crystal appears to induce a hardening of the effective breather potential that, however, gets softened at larger deviations. This tendency is imprinted in the change of the first neighbor eigenvectors for breathers with different central-atom differences and frequencies.

Indeed, the eigenvectors for three extreme breather states of the breather band, viz., (i) the breather with $\omega_b = 540$ cm^{-1} and lower central amplitude, (ii) the breather with the highest possible frequency $\omega_b = 578$ cm^{-1}, and (iii) the breather with $\omega_b = 540$ cm^{-1} but larger central amplitude are quite different. While in all three cases the direction of

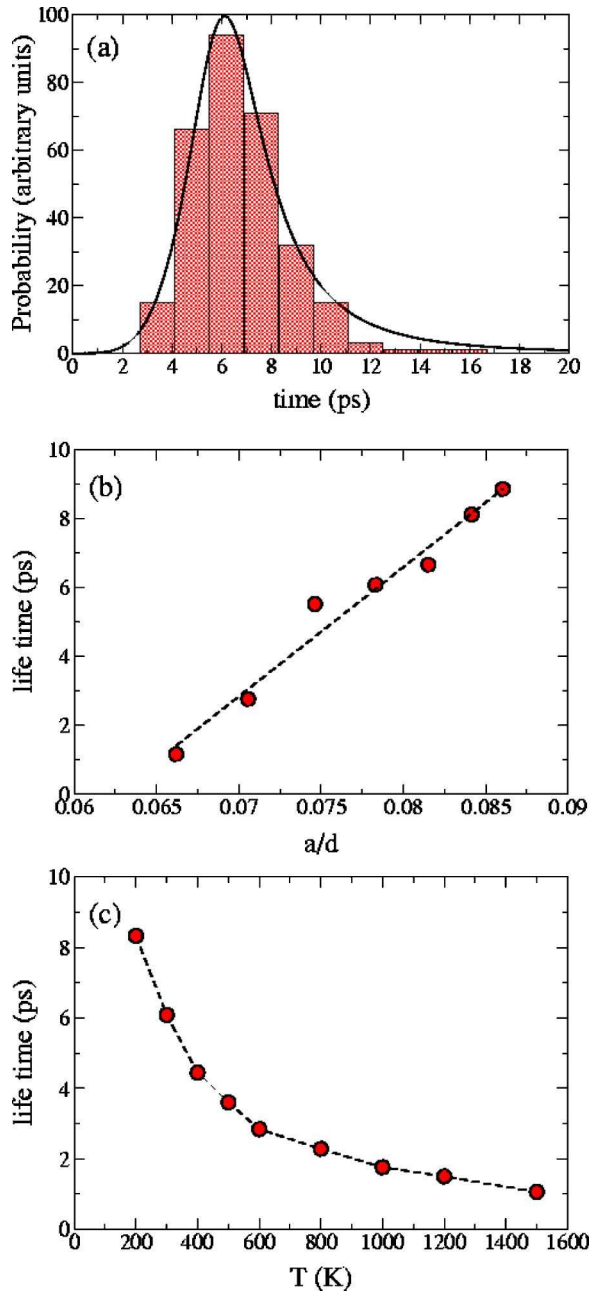

FIG. 3. (a) Probability distribution (unnormalized) of breather lifetime at $T=300$ K. (b) Breather lifetime as a function of distortion of the central atoms at $T=300$ K. (c) Breather lifetime as a function of temperature. For (a) and (c), the breather frequency is $\omega_b=578$ cm^{-1} and corresponds to the top of the breather band (see Fig. 2).

the central-atom eigenmode does not change, in the first case (i) the first and second neighbor atom eigendirections are approximately parallel to the one defined by the central two atoms while as the amplitude increases and we move towards breathers (ii) and (iii), this direction becomes closer to being perpendicular to it. As a result we observe that the lower branch of the DB frequency-amplitude curve is dominated by angular motion of the second and third neighbors resulting in the formation of an effective cage by the first and second neighbors for the central atoms leading to bond hardening. This cage is progressively removed in the second branch leading to an eventual softening of the bonds and the remarkable frequency degeneracy in the breather states. We note that the breathers with frequency degeneracy found here have distinct eigenstates that differ particularly in the first and second neighbors while, additionally, have completely different energies. All breathers found in this range are stable as we have verified through substitution of the initial breather state in the dynamical equations of motion and subsequent monitoring of the time evolution. However, while breathers in the range $\omega \gtrsim 550$ cm^{-1} have a lifetime over 60 ps we found that for breathers with $\omega \lesssim 550$ cm^{-1} lifetime reduces by almost an order of magnitude.

Having studied the onset of localization in the purely Hamiltonian case, we now turn our attention to the DB properties at finite temperatures. To this effect we consider our silicon lattice model with kinetic terms thermalized to a given temperature T and superimpose on it our precise breather state found in the way outlined above. We evolve the system in time and measure the decay time concentrating primarily in the central two silicon atoms. In order to take into account the statistical fluctuations of the process we repeat this procedure several times to construct a histogram describing the probability of breather decay as a function of time, such as the one shown in Fig. 3(a) for $T=300$ K. We note that the breather decay distribution is not a Gaussian but has Gaussian features although it has a clear tail at long times; it can be fitted by a power-law distribution of the form $A_0x^4/[(x-A_1)^8+A_2]$, with A_0, A_1, and A_2 appropriate constants. Due to the specific power-law-like shape of the distribution we choose to define as breather lifetime the time associated to the mode, i.e., the most probable value of the distribution, that, in the depicted case is equal to $\tau_b = 6.1$ ps.

Clearly, the breather lifetime for each temperature depends on the specific breather studied. In Fig. 3(b) we plot the breather lifetime at $T=300$ K as a function of the breather amplitude of the central atoms; we note that DB lifetime increases linearly with central displacement or frequency, indicating that, once generated, the more energetic breathers survive longer. Systematic study in the way presented previously of the breather lifetime as a function of temperature results in the curve of Fig. 3(c) that applies to breathers in the center of the breather band. We note that although the DB lifetime decays to ≈ 2 ps at temperatures 800 K and higher the state does not completely disappear even at 1500 K. We find thus that breathers once generated are very robust to temperature fluctuations.

In addition to silicon we performed similar studies to other valence-four atomic models, viz., those of germanium and carbon. For germanium we found analogous behavior, viz., existence of a breather band above the phonon zone end separated by a small breather gap. In the case of carbon, however, we were not able to construct breathers in a way similar to that of silicon and germanium. We evaluated numerically the interaction energy of the central two atoms as function of distance and found that while in the case of Si

and Ge this energy differs very little in the case of C there is a substantial increase by more than 100% in the regions where breathers could form. Thus, although we also observe a bond hardening for C, the reason for no breather formation may be linked to the fact that the much larger effective intercarbon coupling moves the system away from the region of the anticontinuous limit where breathers can exist,[18] and as a result does not enable the formation of localized modes in this spectral region. In order to test the validity of Tersoff results away from the linear regime we also checked the possibility for breather mode construction using other semiempirical forms for silicon.[19,20] Due to the fact that these potentials are either soft[19] or lead to essentially linear pair atomic forces[20] in the regions of interest no long-lived stable breather modes could be constructed. In what regards finally experimental realizations of intrinsic localization, our findings would be compatible with a $\mathbf{k}=\mathbf{0}$ phonon optic-mode local hardening in some temperature range. Although Raman spectra in crystalline[21] and nanocrystalline[22] Si show a general mode softening with temperature, some small but discernible deviations that are noted especially in the nanocrystalline case where the effective system nonlinearity is substantially enhanced may be connected with our findings.

In conclusion, we have presented a computational analysis of nonlinear localization in diamond structures of silicon, germanium, and carbon using Tersoff potentials. For the first two elements we found a breather band above the phonon band while for carbon no such band was identified. Frequency degeneracy in breathers was found due to the effective formation of a breather cage from the second and third neighbor atoms that leads in the specific pseudopotentials to an effective potential hardening in a limited range of distances. The breather lifetime at finite temperatures was calculated and found to be of order 6 ps at $T=300$ K whiledecays to ≈ 2 ps at temperatures higher than 800 K. We note that we were not able, however, to construct breathers using other standard pseudopotentials and, as a result, further investigations are needed both in assessing the regime of validity of pseudopotentials in the nonlinear regime as well as the actual experimental realization of nonlinear localized modes in valence-IV semiconductors.

This research was supported in part by the European Union under Contract No. HPRN-CT-1999-00163.

[1] A.J. Sievers and S. Takeno, Phys. Rev. Lett. **61**, 970 (1988).
[2] Chaos **13**, 586 (2003), special issue on nonlinear localized modes, edited by Y. Kivshar and S. Flach.
[3] R.S. MacKay and S. Aubry, Nonlinearity **7**, 1963 (1994).
[4] Ding Chen, S. Aubry, and G.P. Tsironis, Phys. Rev. Lett. **77**, 4776 (1996).
[5] G.P. Tsironis and S. Aubry, Phys. Rev. Lett. **77**, 5225 (1996); A. Bikaki, N.K. Voulgarakis, S. Aubry, and G.P. Tsironis, Phys. Rev. E **59**, 1234 (1999).
[6] W.Z. Wang, J. Tinka Gammel, A.R. Bishop, and M.I. Salkola, Phys. Rev. Lett. **76**, 3598 (1996).
[7] E. Trias, J.J. Mazo, and T.P. Orlando, Phys. Rev. Lett. **84**, 741 (2000).
[8] P. Binder, D. Abraimov, A.V. Ustinov, S. Flach, and Y. Zolotaryuk, Phys. Rev. Lett. **84**, 745 (2000).
[9] M. Sato, B.E. Hubbard, A.J. Sievers, B. Ilic, D.A. Czaplewski, and H.G. Craighead, Phys. Rev. Lett. **90**, 044102 (2003).
[10] B.I. Swanson, J.A. Brozik, S.P. Love, G.F. Strouse, and A.P. Shreve, Phys. Rev. Lett. **82**, 3288 (1999); N.K. Voulgarakis, G. Kalosakas, A.R. Bishop, and G.P. Tsironis, Phys. Rev. B **64**, 020301(R) (2000); G. Kalosakas, A.R. Bishop, and A.P. Shreve, *ibid.* **66**, 094303 (2002).
[11] S.A. Kiselev and A.J. Sievers, Phys. Rev. B **55**, 5755 (1997).
[12] J.D. Kress, A. Saxena, A.R. Bishop, and R.L. Martin, Phys. Rev. B **58**, 6161 (1998).
[13] G. Kopidakis and S. Aubry, Physica B **296**, 237 (2001).
[14] J. Tersoff, Phys. Rev. Lett. **56**, 632 (1986); Phys. Rev. B **39**, 5566 (1989).
[15] P.C. Kelires, Phys. Rev. Lett. **75**, 1114 (1995); P.C. Kelires and E. Kaxiras, *ibid.* **78**, 3479 (1997); G. Hadjisavvas, G. Kopidakis, and P.C. Kelires, Phys. Rev. B **64**, 125413 (2001).
[16] N. K. Voulgarakis, G. Archontis, S. Skourtis, and G. P. Tsironis (unpublished).
[17] S. Flach, K. Kladko, and R.S. MacKay, Phys. Rev. Lett. **78**, 1207 (1997); G. Kalosakas, S. Aubry, and G.P. Tsironis, Phys. Rev. B **58**, 3094 (1998).
[18] J.L. Marin and S. Aubry, Nonlinearity **9**, 1501 (1994).
[19] F.H. Stillinger and T.A. Weber, Phys. Rev. B **31**, 5262 (1985).
[20] J.F. Justo, Martin Z. Bazant, and Efthimios Kaxiras, Phys. Rev. B **58**, 2539 (1998).
[21] T.R. Hart, R.L. Aggarwal, and B. Lax, Phys. Rev. B **1**, 638 (1970); M. Balkanski, R.F. Wallis, and E. Haro, *ibid.* **28**, 1928 (1983); J. Menendez and M. Cardona, *ibid.* **29**, 2051 (1984).
[22] P. Mishra and K.P. Jain, Phys. Rev. B **62**, 14 790 (2000); M.J. Konstantinovic, S. Bersier, X. Wang, M. Hayne, P. Lievens, R.E. Silverans, and V.V. Moshchalkov, *ibid.* **66**, 161311 (2002).